World Academy of Science, Engineering and Technology
International Journal of Aerospace and Mechanical Engineering
Vol:11, No:6, 2017

Finite Element Modeling of Stockbridge Damper and Vibration Analysis: Equivalent Cable Stiffness

Nitish Kumar Vaja, Oumar Barry, Brian DeJong

***Abstract*—**Aeolian vibrations are the major cause for the failure of conductor cables. Using a Stockbridge damper reduces these vibrations and increases the life span of the conductor cable. Designing an efficient Stockbridge damper that suits the conductor cable requires a robust mathematical model with minimum assumptions. However it is not easy to analytically model the complex geometry of the messenger. Therefore an equivalent stiffness must be determined so that it can be used in the analytical model. This paper examines the bending stiffness of the cable and discusses the effect of this stiffness on the natural frequencies. The obtained equivalent stiffness compensates for the assumption of modeling the messenger as a rod. The results from the free vibration analysis of the analytical model with the equivalent stiffness is validated using the full scale finite element model of the Stockbridge damper.

***Keywords*—**Equivalent stiffness, finite element model, free vibration response, Stockbridge damper.

NOMENCLATURE

d	Diameter of messenger
E	Young's modulus
I	Area moment of inertia
J	Rotational inertia
L	Length of cable
m	Mass of messenger per unit length
M	Mass of counterweight
T	Kinetic energy
V	Potential energy
W	Transverse displacement
E_{eq}	Equivalent Young's modulus
f_c	Frequency with messenger as cable
f_r	Frequency with messenger as rod
I_c	Area moment of inertia of the cable
I_r	Area moment of inertia of the rod
m_c	Mass of messenger as a cable
m_r	Mass of messenger as a rod
ω	Natural frequency

I. INTRODUCTION

POWER lines are often exposed to winds with speeds up to 7 m/s, which cause vortex shedding [1]. The continuous force exerted by the wind causes the conductor to vibrate at a frequency of 3 to 150 Hz. Such vibrations are characterized by small amplitudes [2] and are referred to as "Aeolian Vibration". Uncontrolled Aeolian vibrations might lead to catastrophic failure of power lines [3] as continuous vibration causes bending and tensile stresses in the conductor [4]. Stockbridge dampers are used to control these vibrations.The Stockbridge damper was first developed by George H. Stockbridge in 1925 [5]. The damping mechanism is observed as the vibrations of the conductor are transferred to the Stockbridge damper, and the energy of the conductor is imparted to the oscillating counterweights [6], [7]. The symmetric Stockbridge damper exhibits two resonant frequencies while the asymmetric Stockbridge damper has four [8], [9]. Conventional mathematical models of the Stockbridge damper assume the system to be a 2 DOF system [10], [11] with the counterweight to be a lumped mass and the messenger to be a massless beam. Other nonlinear models [12], [13] use the energy method to model the system. However the latest approach by Barry et.al considers the counterweight as a mass with rotational inertia and employs the bending stiffness of the messenger [14]. A similar mathematical model is developed in this this work using Hamiltons principle to derive the governing system equations.

N. K. Vaja is with the School of Engineering and Technology, Central Michigan University, Mt. Pleasant, MI, 48859 USA (e-mail: vaja1n@cmich.edu).

O. Barry and B. P. DeJong are with the School of Engineering and Technology, Central Michigan University, Mt. Pleasant, MI, 48859 USA.

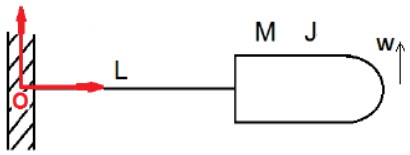

Fig. 1 Schematic of a cantilever beam with a tip mass

II. SYSTEM DESCRIPTION

The Stockbridge damper consists of two masses connected by a messenger with a clamp in its mid-span. For mathematical simplicity, the half model of the Stockbridge damper is analyzed. This model behaves as a cantilever beam with a tip mass. The messenger is a bunch of metal strands knit together to form a cable [8]. The cable is made of galvanized steel. Grey cast iron is used for the counterweight, while aluminum alloy is used for the clamp to reduce its weight [15]. The schematic of the system is depicted in Fig. 1.

III. EQUATION OF MOTION

The reference frame is attached to the clamp, since it is considered as the fixed end of the cantilever beam. The kinetic and potential energies of the system are given by (1) and (2).

$$T = \frac{1}{2}m\int_0^L \dot{W}^2(x,t)dx + \frac{1}{2}M\dot{W}^2(L,t) \tag{1}$$

$$V = \frac{1}{2}EI\int_0^L W''^2(x,t)dx \tag{2}$$

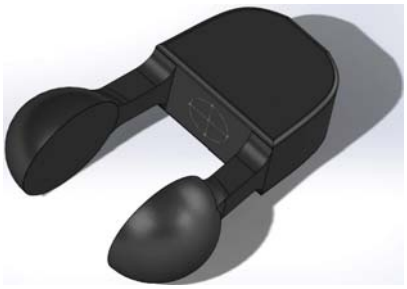

Fig. 2 Model of the counterweight

Fig. 3 Model of the cable

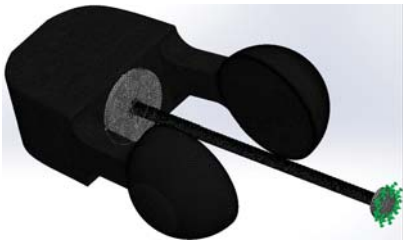

Fig. 4 Meshed model

Here the primes represent differentiation with respect to the axial coordinate x and dots denote the differentiation with respect to time. Using Hamilton's principle, the equation of motion of the system is obtained as the following:

$$EIW^{IV} + m\ddot{W} = 0 \tag{3}$$

Assuming the system exhibits harmonic motion,

$$W(x,t) = y(x)e^{i\omega t} \tag{4}$$

Substituting (4) into (3), the following non dimensional equation is obtained:

$$Y^{IV}(\xi) - \Omega^4 Y(\xi) = 0 \tag{5}$$

where, $y = YL$, $x = \xi L$, $\Omega^4 = \frac{m\omega^2}{EI}L^4$ and the shape function of the system is written as the following:

$$Y = c_1 \sin\Omega\xi + c_2 \cos\Omega\xi + c_3 \sinh\Omega\xi + c_4 \cosh\Omega\xi \tag{6}$$

The boundary conditions are given as:

$$Y(0) = Y'(0) = 0;$$

$$Y''(\xi) = \gamma\Omega^4 Y(\xi);\ Y'''(\xi) = -\alpha\Omega^4 Y'(\xi)$$

where $\gamma = \frac{J}{mL^3}$; $\alpha = \frac{M}{mL}$, the characteristic equation of the system is obtained by substituting the boundary conditions in the shape function

$$\gamma\alpha\Omega^4(cch-1)+\gamma\Omega^3(sch+cch)+\alpha\Omega(sch-csh)-1-csh = 0 \tag{7}$$

where $s = sin\omega\xi$, $c = cos\omega\xi$, $sh = sinh\omega\xi$, $ch = cosh\omega\xi$.

IV. Finite Element Modeling

A half model of Stockbridge damper is developed using SolidWorks. The counterweight, messenger, clamp, and bushing are modeled independently and the assembly is meshed. Two models are developed: one with the messenger as a stranded cable and the other with the messenger as a rod. The stranded messenger is modeled as a 1x19 cable, and it is ensured that there is frictionless contact between the surfaces of individual strands [8]. The messenger is made of galvanized steel with Young's modulus 2.00E+11 N/m^2, Poisson's ratio 0.29 and mass density 7870 kg/m^3.The Young's modulus of the counterweight is 6.62E+10 N/m^2 and its Poisson's ratio was 0.27 with a mass density 7200 kg/m^3.

The modeled parts are assembled and meshed using a curvature based mesh with four Jacobian points. The maximum element size is 1.09424 mm while the minimum element size is 0.218848 mm. The total nodes are 1,712,657 and total elements are 1,111,750.

The rotational moment of inertia of the counterweight is 0.002087 kgm^2 and its mass is 1.1298 kg. The length of the messenger is 0.130 m. A frequency response analysis is conducted on both of the models, and the results are tabulated in Table I.

TABLE I
First 10 Frequencies of Two Models With $d = 5.04mm$

Mode No.	Strand(rad/s)	Rod(rad/s)	Ratio(f_c/f_r)
1	18.801	3.817	0.147547
2	20.204	3.938	0.147693
3	56.103	11.480	0.152579
4	78.952	15.324	0.150305
5	89.126	17.169	0.150216
6	487.920	266.230	0.405206
7	902.770	266.370	0.274766
8	984.950	266.400	0.247847
9	1093.100	266.420	0.205202
10	1538.000	266.430	0.163470

V. Results

The frequency ratio for each model is calculated. In the first case (Case 1), the diameter of the messenger is 5.04 mm. The other four cases are obtained by increasing the diameter of the messenger by 2.5 mm for each case. All the other parameters (counterweight mass and messenger length) are kept the same. The average of the ratios are presented in Table II. These ratios were used to conduct regression analysis and to calculate the equivalent Young's modulus of the stranded cable.

The frequency ratios are plotted against the diameter of the messenger in Fig. 9. Using regression analysis, a relation between the frequency ratio and the diameter of the messenger is obtained as:

$$f_{ratio} = -0.0005d^2 + 0.0067d + 0.1222 \tag{8}$$

The area moment of inertia of a circular cross section is simple to calculate, but the area moment of inertia of the cable with complex cross sectional area is more difficult to calculate.

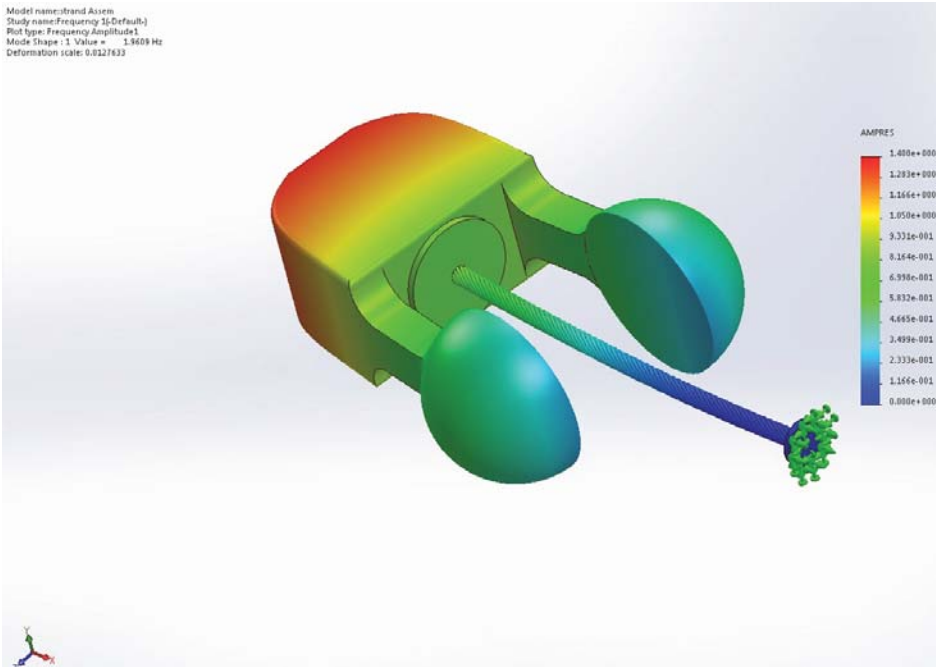

Fig. 5 First mode shape: f =1.96Hz

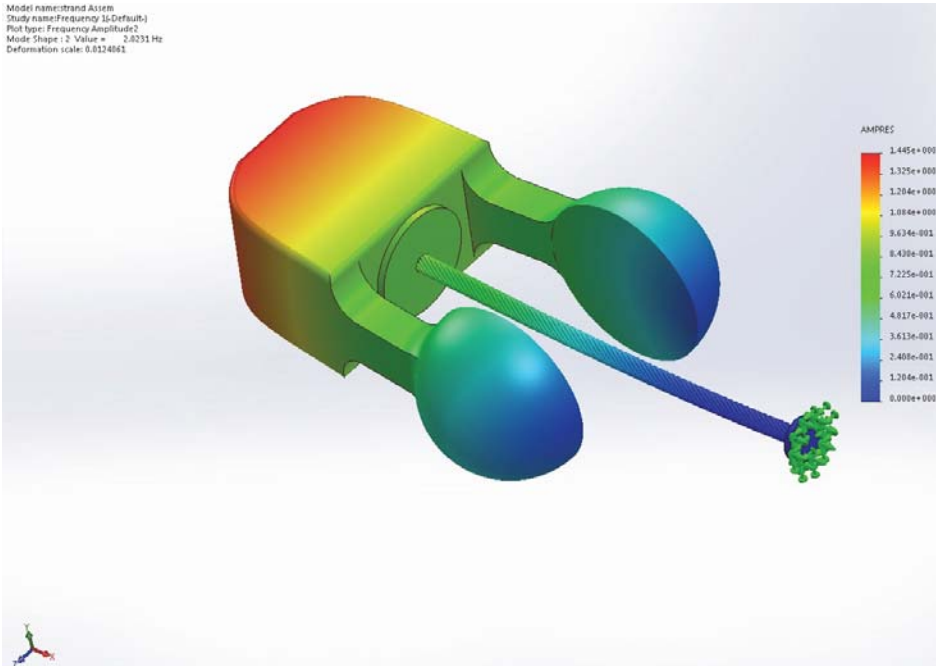

Fig. 6 Second mode shape: f = 2.02Hz

The moment of inertia of cable and rod of different diameters is presented in Table III. It is observed that the moment of inertia of the cable was proportional to moment of inertia of the rod and the relation is presented by (9).

$$0.71 I_r = I_c \tag{9}$$

The equivalent Young's modulus is obtained in terms of the diameter and it is presented in (10).

$$E_{eq} = 3.24 \frac{E}{I_{ratio}} (-0.0005d^2 + 0.0067d + 0.1222)^2 \tag{10}$$

where I_{ratio} is the ratio of I_c and I_r. This ratio is equal to 0.71 as given in (9). E is the Young's modulus of the material (2E+11 N/m^2). The deduced equivalent stiffness is used in the analytical model to calculate the natural frequencies, which are then compared with the numerical model. Fig. 10 shows that

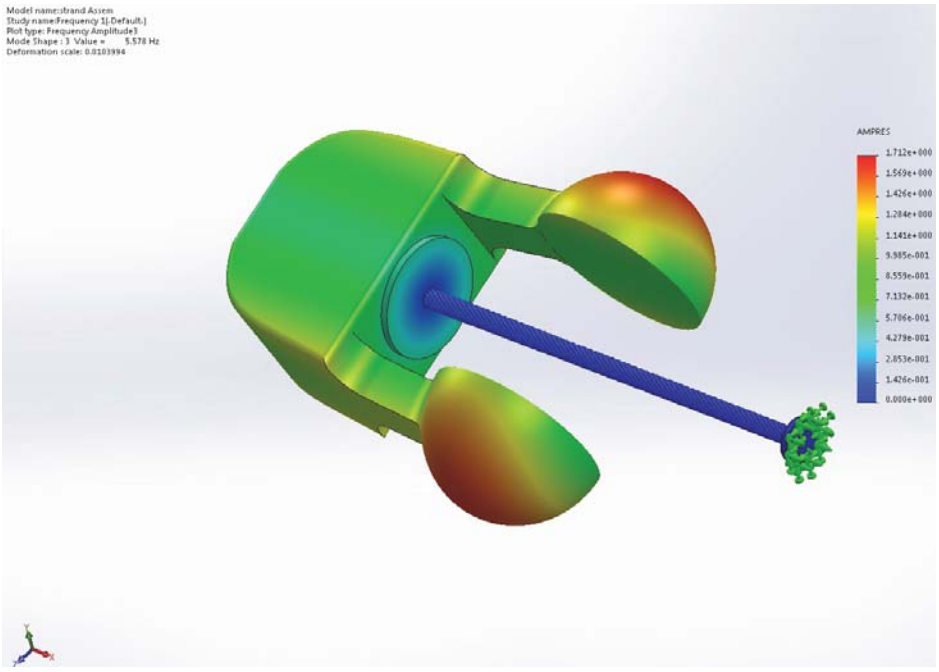

Fig. 7 Third mode shape: f =5.57Hz

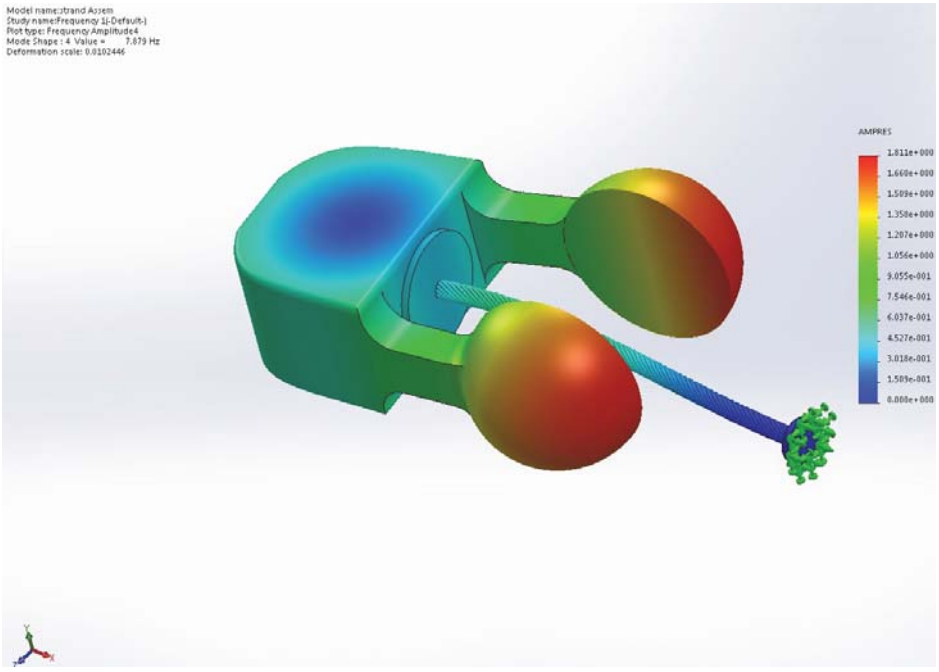

Fig. 8 Fourth mode shape: f =7.87Hz

the results from the analytical model are in good agreement with the results from the numerical model.

VI. Conclusion

The observations from this paper will enable designers to obtain the equivalent stiffness of a stranded cable with reference to a rod with equal diameter. This would save a lot of energy that is put into experiments for determining messenger bending stiffness, which is both uneconomical and time consuming. The equivalent stiffness could be used in the conventional model and the natural frequencies of the Stockbridge damper could be calculated precisely.

Acknowledgment

Thanks to Central Michigan University for supplying the resources and opportunities to conduct research.

TABLE II
AVERAGE FREQUENCIES OF TWO MODELS AND THEIR RESPECTIVE RATIOS

Diameter(mm)	Average Ratio (f_c/f_r)
5.04	0.143822
6.29	0.145150
7.54	0.150216
8.79	0.144408
10.04	0.145914
11.29	0.139029
12.54	0.133327
13.79	0.124206
15.04	0.122413

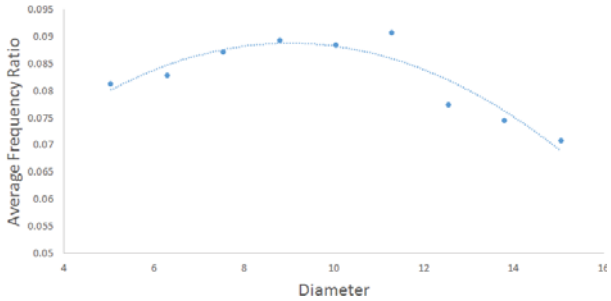

Fig. 9 Regression analysis

TABLE III
COMPARISON OF MOMENT OF INERTIA OF MESSENGER

Case	$I_r(m^4)$	$I_c(m^4)$	Ratio (I_c/I_r)
Case 1	3.16E-11	2.26E-11	7.14E-01
Case 2	1.58E-10	1.14E-10	7.22E-01
Case 3	4.98E-10	3.58E-10	7.19E-01
Case 4	1.21E-10	8.71E-11	7.18E-01
Case 5	2.51E-09	1.80E-09	7.17E-01

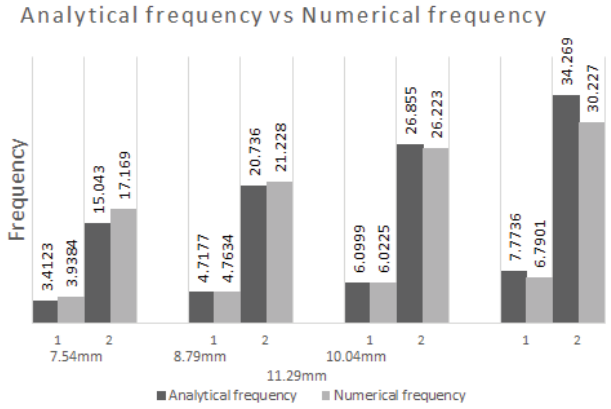

Fig. 10 Comparison between the first two modes for different diameters

REFERENCES

[1] O. M. Griffin and G. H. Koopmann, 1977. The Vortex-Excited Lift and Reaction Forces on Resonantly Vibrating Cylinders, Journal of Sound and Vibration, Volume 54, Issue 3, 8 October 1977, Pages 435-448.
[2] EPRI. 2006. Transmission Line Reference Book, Wind Induced Conductor Motion, Palo Alto, California: Electrical Power Research institute.
[3] D. Havard. 2008. Assessment of the Cowal JCT x Longwood TS for Vibration Control, Toronto, Ontario.
[4] Sauter, D., and P. Hagedorn. On the Hysteresis of Wire Cables in Stockbridge Dampers. International Journal of Non-Linear Mechanics 37.8 (2002): 1453-1459.
[5] G. Stockbridge. 1925. Vibration Damper Patent No.1675391, USA Patent Office.
[6] Schmidt, J. T. and Biedenbach, G. and Krispin, H. J., 1997.Laboratory Measurement of the Power Dissipation Characteristics of Aeolian Vibration Dampers,IEEE Transactions on Power Delivery, Vol. 12, No. 4, October 1997.
[7] Guide on the Measurement of the Performance of Aeolian Vibration Dampers for Single Conductors, IEEE Std. 664-1993, 1993.
[8] Luo, Xiaoyu and Wang, Liang and Zhang, Yisheng, 2014. Nonlinear Numerical Model with Contact for Stockbridge Vibration Damper and Experimental Validation. Journal of Vibration and Control. DOI = 10.1177/1077546314535647.
[9] Oumar Barry, Jean Zu, 2013. Vibration Analysis of Stockbridge Damper: Expiremental Verification. Proceedings of the 24th CANCAM Saskatoon, Saskatchewan, Canada, June 2-6, 2013.
[10] D. Feldman. 2000. Aeolian Vibration: Possible Effects of Non Linear Behaviour of Stockbridge Dampers, Electricite de France.
[11] Wagner, H., Ramamurti, V., Sastry, R., and Hartman, K. 1973. Dynamics of Stockbridge Dampers, Journal of Sound and vibration, vol. 30, pp. 207-220.
[12] Pakdemirli, M., and Nayfeh, A. H., 1994. Nonlinear Vibration of a Beam- Spring-Mass System. ASME J. Vib. Acoust., 166(4), pp. 433438.
[13] Ozkaya, E., 2001. Non-Linear Vibrations of a Simply-Supported Carrying Concentrated Masses. J. Sound Vib., 257(3), pp. 413424.
[14] Oumar Barry, J. W. Zu, D. C. D. Oguamanam, 2015. Nonlinear Dynamics of Stockbridge Dampers.Journal of Dynamic Systems, Measurement, and Control. June 2015, Vol. 137 / 061017-1.
[15] Krispin, H. J. and Fuchs, S. and Hagedorn, P., 2007. Optimization of the Efficiency of Aeolian Vibration Dampers. IEEE PES PowerAfrica 2007 Conference and Exposition Johannesburg, South Africa, 16-20 July 2007.